Food Hydrocolloids 125 (2022) 107427

Contents lists available at ScienceDirect

Food Hydrocolloids

journal homepage: www.elsevier.com/locate/foodhyd

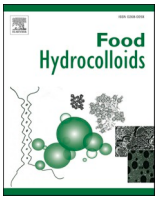

Fractionation methods affect the gelling properties of pea proteins in emulsion-filled gels

Remco Kornet [a,b,1], Simha Sridharan [a,c,1], Paul Venema [b,*], Leonard M.C. Sagis [b], Constantinos V. Nikiforidis [c], Atze Jan van der Goot [d], Marcel B.J. Meinders [e], Erik van der Linden [b]

[a] TiFN, P.O. Box 557, 6700, AN Wageningen, the Netherlands
[b] Laboratory of Physics and Physical Chemistry of Foods, Wageningen University, Bornse Weilanden 9, 6708, WG Wageningen, the Netherlands
[c] Biobased Chemistry and Technology, Wageningen University, Bornse Weilanden 9, 6708, WG Wageningen, the Netherlands
[d] Laboratory of Food Process Engineering, Bornse Weilanden 9, 6708, WG Wageningen, the Netherlands
[e] Food and Biobased Research, Wageningen University and Research, 6700, AA Wageningen, the Netherlands

ARTICLE INFO

Keywords:
Emulsion-filled gels
Pea protein
Plant protein
Rheology
Interfacial properties
Microstructure

ABSTRACT

Plant proteins, after extraction from sources such as pea can be used as functional ingredients in emulsions and gels. However, the protein fractionation route used affects the protein functionality. We investigated the differences in rheological properties of emulsion-filled gel (EFGs) structured by pea protein isolate obtained using either isoelectric precipitation (PPIp) or diafiltration (PPId), at varying pH and oil content. PPIp and PPId had a protein content of 75.3 and 77.7 wt %, respectively. We first studied the oil-water interfacial rheology and composition in emulsions, as these interfacial and emulsion properties can influence EFG properties. Both PPIp and PPId formed a viscoelastic, soft-solid protein layer around the oil droplets and both PPIs were able to stabilize emulsions with monomodal droplet size between 1 and 10 μm. Additional pea protein was added to the emulsions to achieve a final protein dry matter content of 15 wt % and gelling was induced by heating the protein-enriched emulsion in the rheometer to 95 °C. At pH 5, PPIp and PPId formed EFGs with comparable firmness (i.e. similar G') and with a heterogeneous microstructure. At pH 7, PPIp formed less firm and homogeneous gels compared to PPId. The difference was related to protein solubility and aggregation, caused by different fractionation methods. In the EFGs, the presence of oil droplets did not reinforce the gel structure, which could be explained by weak interactions between the oil droplet interface and protein matrix. Our results show that pea protein fractionation routes affect the properties of PPI gels and EFGs. These insights may contribute to pea protein fractionation that is tailored to specific structural requirements for gel-based foods.

1. Introduction

Proteins are used as structuring agents in foods. They can stabilize oil droplets in oil-water mixtures to form an emulsion. Proteins can also be used as gelling agents; in which case they form a space spanning network that incorporates other constituents such as water and oil. In the case of emulsion-filled gels, a small quantity of oil droplets is dispersed in a continuous protein-gel matrix (or polymer gel matrix). In those cases, proteins can serve as an emulsifier to stabilize oil droplets and as gelling agent. To form emulsion-filled gels, excess proteins are usually present in the emulsion system. The excess proteins are triggered to form gels upon e.g. heating, acidification, addition of ions or enzymatic cross-linking (Farjami & Madadlou, 2019). These triggers create cross-links between proteins and between proteins and oil droplets through hydrophobic, electrostatic and chemical interactions, which results in a gel system with oil droplets entrapped. There are a variety of foods that can be classified as emulsion-filled gels, such as yoghurt, cheese, ice cream and processed meat products (Geremias-Andrade, Souki, Moraes, & Pinho, 2016). Most of these products are structured using animal-based proteins. However, the consumption of plant-based foods is rapidly increasing, due to environmental and health concerns. There is thus interest in replacing dairy proteins with plant proteins as structuring

* Corresponding author.
E-mail address: paul.venema@wur.nl (P. Venema).
[1] These authors have contributed equally to this work.

https://doi.org/10.1016/j.foodhyd.2021.107427
Received 9 September 2021; Received in revised form 9 November 2021; Accepted 2 December 2021
Available online 6 December 2021

agents.

Plant proteins, however, have different physicochemical properties than dairy proteins, and often behave differently than their dairy counterparts, for instance, in terms of gelation (Schmitt, Silva, Amagliani, Chassenieux, & Nicolai, 2019) and emulsifying properties (Hinderink, Münch, Sagis, Schroën, & Berton-Carabin, 2019). Different technical solutions have been proposed to solve the challenges related to replacing dairy proteins, including i) enzymatic treatment (Panyam & Kilara, 1996; Zeeb, McClements, & Weiss, 2017), ii) partial replacement of dairy proteins by plant proteins (Jose, Pouvreau, & Martin, 2016; McCann, Guyon, Fischer, & Day, 2018), iii) recombinant dairy proteins (Vestergaard, Chan, & Jensen, 2016) and iv) alternative fractionation routes to influence plant protein functional behaviour (Adenekan, Fadimu, Odunmbaku, & Oke, 2018; Jung, Lamsal, Stepien, Johnson, & Murphy, 2006; Kornet, Veenemans, et al., 2021, p. 106691; Peng, Kersten, Kyriakopoulou, & van der Goot, 2020; Sridharan, Meinders, Bitter, & Nikiforidis, 2020). In this research, we focus on the fractionation routes of plant proteins in the context of emulsion-filled gels.

A commonly reported way of fractionating plant protein is aqueous fractionation, which involves a solubilization step at alkaline pH followed by a precipitation step at acidic pH (Boukid, Rosell, & Castellari, 2021). Alternative methods of fractionation include dry fractionation (Pelgrom, Vissers, Boom, & Schutyser, 2013), salt-extraction (Sun & Arntfield, 2011) and membrane filtration (Alonso-Miravalles et al., 2019). Different fractionation routes yield pea protein isolates with different protein compositions. Upon isoelectric precipitation only pea globulins are recovered, while when replacing isoelectric precipitation with membrane filtration and salt extraction, both pea globulins and albumins were recovered (Makri, Papalamprou, & Doxastakis, 2005; Stone, Karalash, Tyler, Warkentin, & Nickerson, 2015).

Therefore, to obtain both globulins and albumins, salt extraction or membrane filtration techniques may be preferable. Amongst the two, filtration is ideal for obtaining complete plant protein isolates, since it does not require any addition of salt. Moreover, isoelectric precipitation and membrane filtration have been widely used aqueous fractionation routes for plant proteins. The two methods also result in different physicochemical properties and compositions, with diafiltrated pea protein isolates containing both globulins and albumins, and precipitated pea protein isolates only contain (partially aggregated) globulins (Kornet, Shek, et al., 2021, p. 106691). Therefore, in our study, we have investigated proteins obtained by isoelectric precipitation and diafiltration techniques.

Furthermore, besides the effect of fractionation method on the type of proteins that are obtained, the physicochemical properties of each protein class might be affected as well. For instance, membrane filtration leads to pea proteins with a higher solubility than the isoelectric precipitation process (Fuhrmeister & Meuser, 2003; Kornet, Shek, et al., 2021, p. 106691). Besides solubility, an important category of protein functionality that is important in foods, is the emulsifying ability. A few studies have focussed on the effect of different fractionation routes on the emulsion properties of pea proteins. It was found that isoelectric precipitation yielded pea protein that could form smaller droplet sizes in oil-water emulsions, than those obtained by salt extraction and membrane filtration (Burger & Zhang, 2019; Karaca, Low, & Nickerson, 2011; Makri et al., 2005). Therefore, fractionation routes along with protein purity, composition could affect emulsification properties of plant proteins.

In the light of emulsion-filled gels, a relevant functionality type to consider is the gelling behaviour. For different plant protein sources, it has been reported that the gelling behaviour of proteins was affected by the fractionation method and that this had a larger impact on the gelling behaviour than the protein isolate composition (Kiosseoglou, Doxastakis, Alevisopoulos, & Kasapis, 1999; Papalamprou, Doxastakis, Biliaderis, & Kiosseoglou, 2009). In previous research it was found that using membrane filtration instead of isoelectric precipitation, resulted in a pea protein isolate that could form firm gels, comparable in firmness to whey protein isolate gels (Kornet, Shek, et al., 2021, p. 106691). A similar conclusion was reported for lentil protein isolate (Alonso-Miravalles et al., 2019) and chickpea protein isolate (Papalamprou et al., 2009), where diafiltration yielded protein isolates with better gelling properties than precipitated protein. The differences in gel firmness between isoelectric precipitated and membrane filtrated pea protein are probably related to fractionation process-induced aggregation. Isoelectric precipitation induces protein aggregation, which is also reflected in a lower solubility. These aggregates formed more heterogeneous and less cohesive heat-set gels, as opposed to the proteins obtained by membrane filtration. Membrane filtrated protein was not aggregated and thus showed a higher solubility (Kornet, Shek, et al., 2021, p. 106691). Also in other studies, the solubility of a globular protein such as pea globulin, has been related to its ability to participate in heat-induced protein gel formation (Shand, Ya, Pietrasik, & Wanasundara, 2007; Sikorski, 2001).

The gelling and emulsion properties of pea protein – whether or not in the context of different fractionation routes – have been subject of numerous studies. However, only few studies combine the emulsion and gelling properties of plant protein in the context of different fractionation routes, by focussing on emulsion-filled gels (Kim, Renkema, & Van Vliet, 2001; Schmitt et al., 2019; Tang, Chen, & Foegeding, 2011; Yang, Liu, & Tang, 2013). In this study we aim to understand how fractionation methods affect the emulsion-filled gelling behaviour of pea protein. We investigate the ability of two differently fractionated pea protein isolates to form emulsion-filled gels at different pH and oil content. To form emulsion-filled gels, we added protein to the emulsion and used heat to induce gelation and form a continuous protein network. While building on previous research, we aim to get a mechanistic understanding of the relation between fractionation processes and emulsion-filled gelling capacity of pea protein. The new insights obtained may facilitate the development of plant-based food products such as cheese alternatives and meat analogues, by tailoring the fractionation method to specific product requirements.

2. Material and methods

2.1. Materials

Yellow pea (Pisum sativum L.) seeds were acquired from Alimex Europe BV (Sint Kruis, the Netherlands). Rapeseed oil was provided by Danone Nutricia Research (Utrecht, the Netherlands). Chemicals and CLSM dyes were obtained from Merck (Darmstadt, Germany). All samples were prepared with deionized water.

2.2. Methods

2.2.1. Pea protein fractionation

Prior to fractionation, the frozen yellow pea seeds were broken with a pin mill (LV 15M Condux-Werk, Germany) and subsequently milled (ZPS50 impact mill Hosokawa-Alpine, Germany) into flour with a mean particle size of ~100 μm. Two pea protein isolates (PPI) were prepared from the pea flour: one using isoelectric precipitation (PPIp) and the other one using diafiltration (PPId). The fractionation methods are from previous work (Kornet, Shek, et al., 2021, p. 106691) and are briefly described below and a schematic overview is given in Fig. 1.

PPIp was obtained using isoelectric precipitation. First 500 g pea flour was dispersed in 5 L deionized water (1:10 ratio) for 2 h at room temperature, with a pH adjusted to 8 using 1 M NaOH. The flour dispersion was subsequently centrifuged (10000 g, 30 min, 20 °C) to remove solids. The supernatant was brought to pH 4.5 with 1 M HCl to precipitate the pea globulins. After 2 h of stirring at room temperature, the precipitated proteins were separated by centrifugation (10000 g, 30 min, 20 °C). The protein-rich pellet was re-dispersed at pH 7 and freeze-dried afterwards.

PPId was obtained without any pH adjustments and fractionation

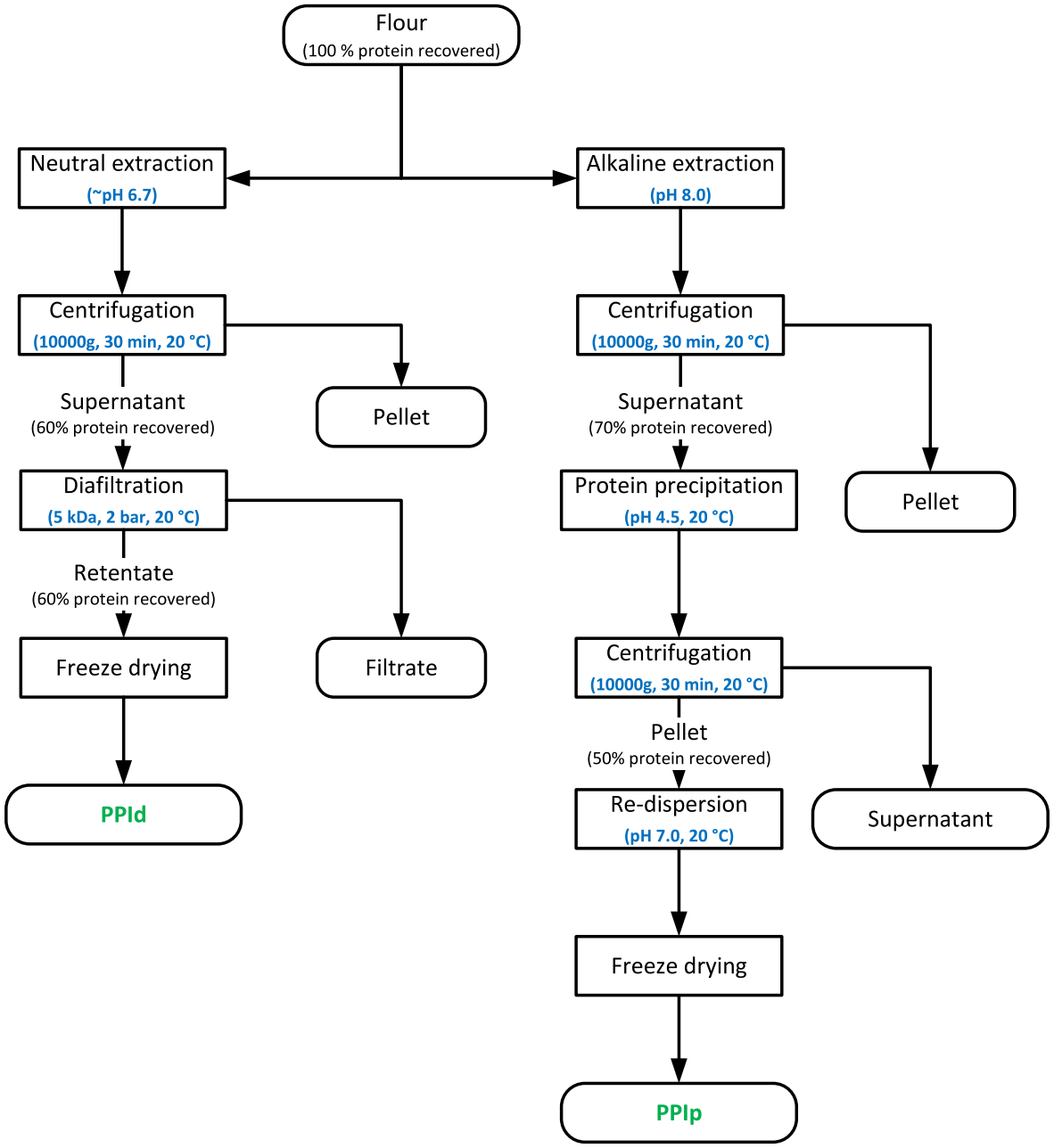

Fig. 1. Schematic overview of the two fractionation processes. The left process used neutral extraction and diafiltration to yield PPId and the right process uses alkaline extraction and isoelectric precipitation to yield PPIp. The protein recovery data originate from previous studies (Kornet, Shek, et al., 2021, p. 106691; Kornet et al., 2021, p. 106891).

was achieved by diafiltration instead. 500 g pea flour was dispersed in 5 L deionized water (1:10 ratio) and stirred for 2 h at room temperature with the pH left unadjusted (~pH 6.7). Then the dispersion was centrifuged at 10000 g for 30 min and the supernatant was collected and further fractionated by ultrafiltration and diafiltration at room temperature with a Sartocon Slice crossflow set, consisting of a SartoJet pump, Sartocon Slice filter holder, pressure gauges and valves, all connected via sanitary Tri Clamp adapters (Sartorius AG, Goettingen, Germany). Two Sartocon Slice cassettes with a 5 kDa Hydrosart membrane (Sartorius AG, Goettingen, Germany) were applied at a transmembrane pressure of 2 bar. The cellulose-based membranes were non-protein binding and had a filter area of 2 × 0.1 m2. At the start of the filtration process the supernatant was diluted with an equivalent amount of water. The supernatant was then concentrated using ultrafiltration up to a concentration factor of 2. During diafiltration the filtrate, with mostly sugars and peptides, was discarded and the retentate was recirculated. To maintain diafiltration efficiency, water was added when the retentate became too concentrated, eventually leading to a total diafiltration factor of about 8. After diafiltration the concentrated retentate was collected and freeze-dried.

The freeze-dried pea protein isolates were stored at −18 °C. The nitrogen content was measured with a Flash EA 1112 series Dumas (Interscience, Breda, the Netherlands) and used to calculate the protein content (with a nitrogen-conversion factor of 5.7). The protein content of the freeze dried PPIp was found to be 75.3 (±0.7) wt. % and PPId 77.7 (±0.4) wt. %. The protein recovery of the precipitation and diafiltration process has previously been reported to be 52 (±7.3) and 63 (±63) %, respectively (Kornet, Shek, et al., 2021, p. 106691; Kornet et al., 2021). The ash content of PPIp and PPId was previously measured to amount 4.6 (±0.4) and 5.9 (±0.1) wt. %, respectively (Kornet, Shek, et al., 2021,

p. 106691). PPIp was significantly higher in Na^{+} than PPId (1.6 and 0.1 wt %, respectively), but lower in multivalent ions such as Ca^{2+}, Mg^{2+}, Mn^{2+} and Zn^{2+}. The complete mineral composition of the PPIs is reported in Table 2 of Kornet, Shek, et al. (2021). Other impurities include sugars (<3 kDa) and residual moisture (Kornet et al., 2020).

2.2.2. Interfacial tension and dilatational rheology

The interfacial tension reduction and dilatational rheology of the oil–water interface stabilized by pea protein was measured with an automated drop tensiometer (Tracker, Teclis Instruments, Tassin, France). Dispersions of PPIp and PPId containing 0.01 wt % were prepared in deionized water and the pH was adjusted to pH 7. The dispersion could solubilize under magnetic stirring for 3 h.

Rapeseed oil was treated with Florisil overnight to remove impurities and was used as the oil phase in the emulsions. In brief, a 1:3 (w/w) ratio of Florisil to oil was mixed overnight and centrifuged the next day to obtain contaminant-free oil, which was used in the interfacial study.

In the drop tensiometer, a droplet of the stripped rapeseed oil with 20 mm^2 area was created at the tip of a J-shaped needle, in a clean 7 mL optical glass cuvette filled with the aqueous protein solution. The needle was fitted to a 500 μL syringe. The shape of the oil droplet was monitored continuously with a camera. From this shape the interfacial tension was calculated by the Wdrop® software from Teclis® Instruments (Tassin, France). The dynamic interfacial tension reduction profile was monitored continuously for 2 h and plotted against time.

After 2 h of interfacial tension measurement, dilatational viscoelasticity was measured by changing the surface area of the droplet in a sinusoidal manner. The droplet was subjected to changes in surface area with amplitudes of 5%, 10% and 15% deformation with respect to the initial surface area (20 mm^2). Each amplitude was applied for 50 s with five subsequent cycles. This was followed by 250 s of rest period before the next higher amplitude was applied. The interfacial tension change and change in area were recorded during the oscillation, and the dilatational elastic (Ed') and viscous moduli (Ed″) were obtained from the intensity and phase of the first harmonic of the frequency spectrum (obtained by FFT of the interfacial tension signal).

2.2.3. Emulsion preparation for emulsion-filled gels

The aim was to produce emulsion-filled gels (EFGs) with final oil concentration of 10 wt %, 20 wt % and 30 wt %, using PPIp or PPId dispersions. These oil contents are of the same order as in e.g., cheese. To obtain this final concentration in EFGs, first, emulsions with 11.56 wt %, 22.7 wt %, and 33.5 wt % oil concentrations were prepared, respectively. The protein to oil ratio was kept constant at 1 g protein/50 g oil by adjusting the concentration of proteins in the aqueous phase. This protein to oil ratio was used based on previous work, where a 1:50 wt ratio protein to oil was found to be sufficient to cover the oil droplet interface (Sridharan et al., 2020).

Firstly, the required amount of proteins was dispersed in deionized water. Then the pH was adjusted to pH 7, using 0.5 M NaOH, and allowed to stir for 3 h under magnetic stirring. The dispersions were then sheared for 15 s at 6000 rpm in an IKA (Ultra-Turrax, IKA, Staufen, Germany) Ultra-Turrax using a dispenser of rotor diameter 12.7 mm and gap between rotor and stator of 0.3 mm. Subsequently, rapeseed oil was added slowly, while the mixtures were sheared for another 60 s at 10000 rpm to produce a coarse emulsion. The formed coarse emulsions were further homogenized by passing through a GEA (Niro Soavi NS 1001 L, Parma, Italy) high pressure homogenizer for five passes with a homogenization pressure between 250 and 350 bars. A higher pressure was used for a higher oil content to obtain similar droplet sizes. When similar droplet size is envisioned with higher oil content, an increase in the surface area of oil droplets occurs. Therefore, a higher shear input is necessary to the system and therefore, we used higher pressure for a higher oil content. Detailed compositions are given in Table 1.

Table 1
Final emulsion composition and emulsification pressure for emulsions stabilized by PPIp (precipitated) and PPId (diafiltrated).

Oil content (wt. %)	Protein content (wt. %)	Homogenization pressure
11.56	0.2	250
22.7	0.4	300
33.5	0.6	350

2.2.4. Static light scattering

The individual droplet size of the emulsions was measured with laser diffraction in a Malvern Mastersizer® 3000 (Malvern® Instruments Ltd., Malvern, U.K.). The samples were dispensed with a hydrodispenser®, and the droplet size was represented by the volume mean diameter ($D_{4,3}$).

To measure individual droplet sizes, the emulsions were treated with 1 wt % SDS solution. Addition of SDS breaks droplet aggregation driven by non-covalent protein interaction, so the size of individual oil droplets could be measured in this manner (Tangsuphoom & Coupland, 2008). Equal volumes (1 mL) of emulsion and 1 wt % SDS solution were mixed, and the size was immediately calculated by the Malvern Mastersizer software, with the refractive index set to 1.47.

2.2.5. Sodium dodecyl sulphate polyacrylamide gel electrophoresis (SDS-PAGE)

SDS-PAGE was conducted to qualitatively analyse the protein classes that are present in the pea protein isolates and at the interface of the emulsion oil droplets. The protein isolates were prepared by weighing dry protein powder directly and dissolving in the appropriate SDS buffer as explained below. In order to separate the oil droplets in the emulsion samples, first the emulsions were centrifuged. About 12 mL of emulsions were centrifuged at 10,000 g for 30 min at 4 °C. The cream layer was removed and re-suspended in water at 1:10 wt ratio. Then, another centrifugation at 3000*g* for 15 min at 4 °C was conducted. The cream layer after centrifugation was collected, labelled as the 'em' phase and the oil droplet free aqueous phase was collected, labelled as 'aq' phase.

The samples (i.e. em phase and aq phase) were dispersed in 250 μL NuPAGE® LDS sample buffer and about 750 μL deionized water was added so that the final protein concentration was about 2 mg/mL. The samples were subsequently heated at 90 °C for 15 min followed by centrifugation at 425*g* for 1 min. Next, 20 μL of the supernatants were loaded into the wells of a NuPAGE® 4–12 wt % Bis-Tris precast gel. A protein standard (10 μL) (10 kDa–200 kDa) was also loaded and the gel was fixed in the electrophoresis chamber. After filling the chamber with MES Buffer, the electrophoresis was run at 200 V for 40 min. Further, the gel was separated and washed with deionized water and was gently shaken for 4 h in Comaisse® blue stain. The gel was then destained with a solution containing 20% ethanol, 50% acetone, 30% water for 4 h. Finally, the gel was washed with deionized water.

2.2.6. Emulsion-filled gels preparation

After the emulsions were formed, additional proteins were added to form the protein enriched emulsions. To the formed PPIp and PPId emulsions, PPIp and PPId were added respectively. The amount of protein added was standardized to a final concentration of 15 wt % in the aqueous phase for all the emulsions (i.e. constant protein-to-water ratio). The pH of the protein enriched emulsions was adjusted to pH 7 or pH 5 and magnetically stirred at 300 rpm for 3 h. The protein-enriched emulsions were transformed into emulsion-filled gels by applying heat. In our study, we investigated the heat-set gelation through a temperature sweep experiment using a rheometer (section 2.2.7).

In this study, we first prepared the emulsions and then added excess proteins before forming emulsion-filled gels. This method was used since in this way we ensured that our emulsions were not highly viscous during emulsification and to better control the eventual protein

concentration in the aqueous phase.

2.2.7. Small amplitude oscillatory shear (SAOS) rheology of gels

The gelling behaviour of the dispersed PPI isolates and the protein-enriched emulsions was examined by temperature sweeps using an MCR302 rheometer (Anton Paar, Graz, Austria) with a sand-blasted concentric cylinder geometry (CC-17). A sand-blasted geometry was used to reduce the chance of wall slip and a solvent-trap was placed on top of the concentric cylinder to reduce solvent evaporation upon heating. The sample was heated from 20 °C to 95 °C with 3 °C/min, kept at 95 °C for 10 min, and cooled to 20 °C with 3 °C/min. To verify that the G′ did not change anymore after the temperature sweep, the sample was kept for another 5 min at 20 °C. Throughout the temperature sweep, an oscillatory deformation was imposed at a constant frequency of 1 Hz and a strain amplitude of 1%, which fell within the linear viscoelastic (LVE) regime of the gel. The recorded response was processed by the Rheocompass software (Anton Paar, Graz, Austria) to calculate the elastic modulus (G') and viscous modulus (G"). All samples were prepared in duplicate.

2.2.8. Medium and large amplitude oscillatory shear (MAOS & LAOS) rheology of gels

The gels formed during the temperature sweep were further characterized by applying non-linear deformation, using the same rheometer and geometry as for the SAOS measurements. The gel was deformed by applying a strain sweep from 0.1 to 1000% in a logarithmic manner, at a constant frequency of 1 Hz and temperature of 20 °C. For each imposed strain amplitude, the oscillating strain, stress and shear rate were recorded. The strain, stress and shear rate values were normalized and elastic and viscous Lissajous plots (i.e. shear stress vs shear strain and shear stress vs shear rate, respectively) were constructed. Also, the elastic and viscous contributions at each strain amplitude were extracted from the Rheocompass software, normalized, and plotted within the Lissajous figures. Lissajous plots were only constructed for the MAOS regime (10–100% strain amplitude), which is the regime where the transition from a predominantly elastic to a predominantly viscous response takes place.

The area that is enclosed within the Lissajous curves represents the dissipated energy per unit volume during an oscillatory cycle. This area thus represents important information from the Lissajous plots, as it reflects the loss of stored energy at a given strain amplitude. When dividing this dissipated energy by the energy dissipated by a perfectly plastic material, the energy dissipation ratio (Φ) is obtained. The energy dissipation ratio can be calculated from the loss modulus (G") and the maximum stress (σ_{max}) at an applied strain amplitude (γ_0) and is determined by Eq. (1) (Ewoldt, Winter, Maxey, & McKinley, 2010).

$$\Phi = \frac{E_d}{(E_d)_{pp}} = \frac{\pi G'' \gamma_0}{4\sigma_{max}} \quad (1)$$

2.2.9. Multi photon microscopy (MPM)

The microstructure of emulsion-filled gels (EFGs) was visualized by using multiphoton microscopy. Multiphoton microscopy differs from a confocal set up in that it uses a low energy near infrared femtosecond laser. The fluorescent molecules are excited by multiple photons of low energy, which enables deeper penetration and reduces photobleaching in the samples (Larson, 2011). Therefore, MPM was used to image deeper into the dense gel samples in our study.

The protein-enriched emulsions (before heating) were stained with 7 μl Nile red (1 mg/mL stock) for oil and 7 μl of Fast green FCF (1 mg/mL stock) for protein. About 60 μL of the stained samples were transferred to a microscope glass slide fitted with a gene frame (Gene frame 65 μL adhesives, Thermo Fisher Scientific, United Kingdom). The gene frames were sealed with a 1.5H cover slip glass and they were placed in a water bath (100 °C, 15 min). The samples were then cooled and visualized using a multiphoton microscope.

The multiphoton microscope is a Leica confocal setup fitted with a Ti: Sapphire laser tuneable from 700 nm to 1080 nm. The samples were imaged at a wavelength of 920 nm using a 40X water immersion objective. The emissions were captured between 480 and 600 nm for Nile red and between 700 and 800 nm for Fast green. Both 2D images and 3D constructs were obtained using a 4 times line averaging sequence. The images were processed using the accompanying Leica® confocal software.

3. Results and discussion

3.1. Emulsion properties

3.1.1. Interfacial properties of PPI dispersions

The gelling and gel properties of emulsion-filled gels (EFGs) are affected by the interaction of the oil droplet interface with the gelled protein matrix (Sala, Van Aken, Stuart, & Van De Velde, 2007) and the droplet stiffness (Van Vliet, 1988). Before studying the emulsion-filled gels, the interfacial tension and rheology and interfacial composition of pea proteins in PPIp and PPId were investigated and compared. Also, the oil droplet size may impact the reinforcement through oil droplets in EFG matrices, as oil droplet stiffness scales inversely with droplet size. Therefore, emulsions were prepared, and their size distributions were measured.

Fig. 2A shows the interfacial tension as a function of time for PPIp and PPId dispersions at the oil-water interface. The faster decrease in the interfacial tension at the beginning indicates that proteins in PPId adsorb at the oil-water interface and reduce the tension faster compared to proteins in PPIp (Beverung, Radke, & Blanch, 1999). The faster adsorption of PPId could be attributed to presence of smaller protein aggregates compared to PPIp, indicating that most proteins are present in a soluble, individual form (Kornet, Shek, et al., 2021, p. 106691), so they can diffuse to the interface. Upon adsorption, these proteins can more easily reconfigure and form an interfacial layer, compared to more aggregated proteins. Previous work has shown that PPId is about 85% soluble at pH 7, while PPIp was only 70% soluble. The lower solubility of PPIp is caused by the partially irreversible aggregation of proteins after isoelectric precipitation. In addition to insoluble aggregates, part of the PPIp protein is present in the form of soluble aggregates (Kornet, Shek, et al., 2021, p. 106691). The fact that more proteins in PPIp exist in an aggregated state, could lead to longer adsorption and rearrangement times before noticeable change in interfacial tension occurs (Beverung et al., 1999). Also due to aggregates being present, the PPIp interfacial tension curve appears noisy, as droplet tensiometry is a visual technique and the presence of aggregates can disturb the measurement resulting in a noisy signal.

The interfacial dilatational rheology of PPIp and PPId were also measured as a function of different amplitudes of dilatation immediately following the interfacial tension measurement. Fig. 2B shows the dilatational elastic moduli (E_d') of PPIp (pink) and PPId (green). PPIp shows an E_d' between 25 and 20 mN/m with a small decrease in E_d' with increasing amplitude. PPId has an E_d' of about 15 mN/m without any amplitude dependency. For both PPIp and PPId, the elasticity is much lower than what was reported for WPI; the latter showed a much higher modulus for the oil-water interface (Perez, Carrara, Sánchez, Santiago, & Patino, 2009). Therefore, the interfaces formed with both pea protein fractions reported here, are relatively weak soft solid-like with limited in-plane protein-protein interactions.

The E_d' of the PPIp stabilized interface is higher than that of a PPId stabilized interface. In other words, PPIp formed a stiffer interface compared to PPId, implying more protein-protein interactions at the interface. PPIp also showed a decrease in E_d' with increasing dilatational amplitude. The amplitude dependency of PPIp could mean that even though the interface of PPIp is firmer at rest, the additional interaction is weak and is disrupted upon increasing amplitude (Ntone et al., 2020). The E_d' of the PPIp stabilized interface showed amplitude dependency,

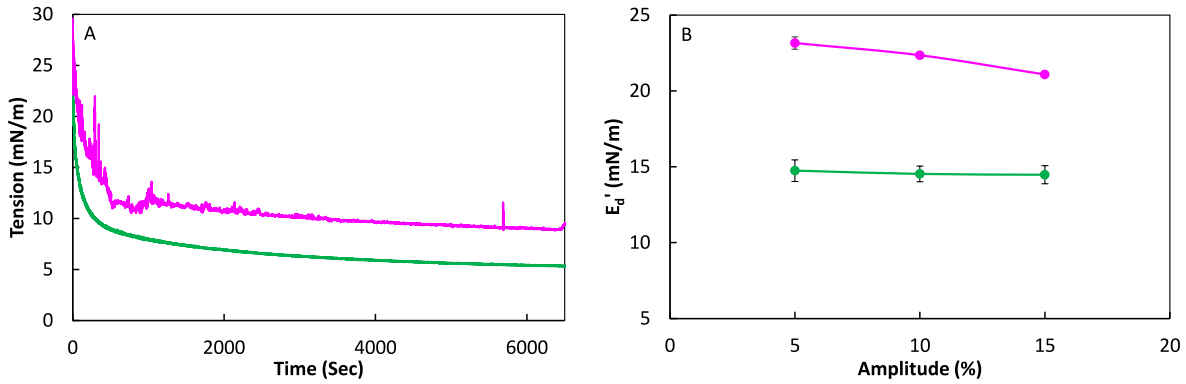

Fig. 2. Interfacial tension measured at the oil-water interface for 0.01 wt% PPIp (—) and PPId (—) measured at 20 °C, pH 7 (A); Dilatational elastic modulus (E_d') as a function of dilatational amplitude for PPIp and PPId measured after 2 h of interfacial tension measurement (B).

while for PPId it did not. To further investigate the interfacial properties, Lissajous figures of the interfacial modulus were plotted and analysed (Sagis & Scholten, 2014). The interfacial Lissajous plots are given in Fig. 3.

Fig. 3 shows the Lissajous plots of surface pressure as a function of relative change in surface area for 5% and 10% amplitudes, and for both PPIp and PPId. The plots from −0.05 to +0.05 along the upward arrow represents the expansion phase and the plot from +0.05 to −0.05 represents compression phase. All four plots show narrow elliptical loops, characteristic of visco-elastic interfaces with a dominant elastic nature (Ntone et al., 2020; Sagis et al., 2014). The PPIp curves at both strain amplitude shows a narrowing effect upon compression (bottom left), which indicates that the response of the interface becomes relatively more elastic upon compression. This shape implies that the proteins at the interface were jammed upon compression, which is consistent with the weak protein-protein interactions (i.e., low E_d'). In PPId curves, the response of the interface was linear with a dominant elastic nature. No narrowing of the loop was visible upon compression, and the resulting

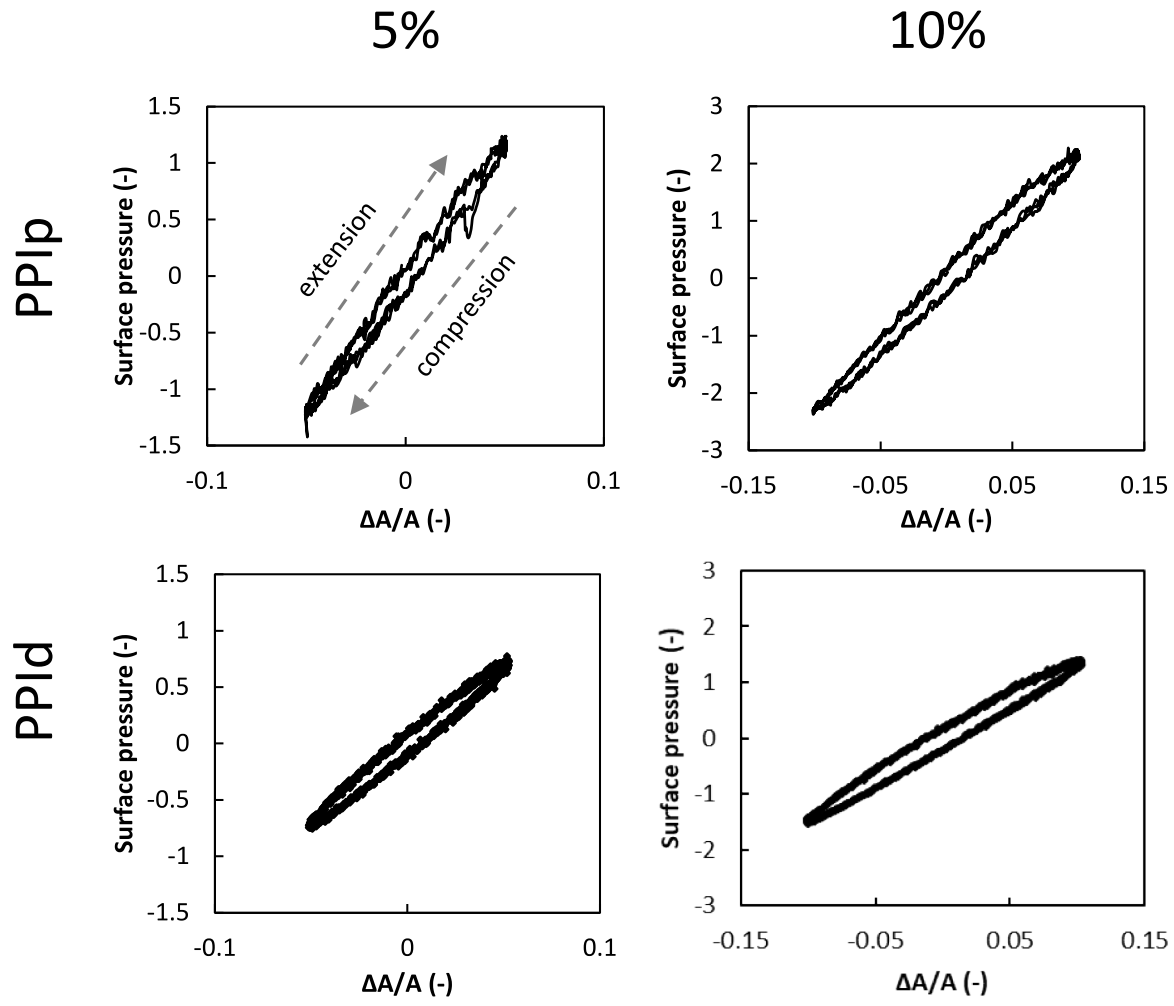

Fig. 3. Interfacial Lissajous plots for 0.01 wt% PPIp (precipitated) (left) and PPId (diafiltrated) (right) dispersion at the oil-water interface obtained from dilatational modulus at 5% and 10% dilatation amplitudes.

interfacial microstructure was significantly stretchable and not affected by the amplitude of deformation. The loops of PPIp showed slightly higher surface pressure than PPId, both upon compression and expansion. This higher surface pressure change in PPIp could be due to stronger interactions occurring compared to PPId. In addition, the dilatational rheology shows decreasing interfacial elasticity in PPIp interfaces and was not observed in PPId. This suggests that the slightly higher stiffness in PPIp interfaces could be due to weak secondary interactions, for example between adsorbed proteins and protein aggregates in the sub-phase which was disrupted due to dilatation of the interface, as seen for rapeseed proteins (Ntone et al., 2020). Overall, the interfacial rheology suggests that both PPIp and PPId formed interfaces with relatively soft solid-like behaviour through weakly interacting protein networks.

3.1.2. Emulsion properties

The droplet sizes of the freshly prepared emulsions were measured to evaluate the emulsifying properties of PPIp and PPId. The size distribution curves of a representative PPIp and PPId emulsion measured with SDS are shown in Fig. 4. The curves for both PPIs show a monomodal size distribution starting around 800 nm up to about 10 μm. Despite the differences in interfacial tension (IFT), the droplet sizes are similar for both emulsions, most likely due to a dynamic emulsification process used compared with the static IFT measurement condition. The similarities in size distributions of oil droplets indicate that the ability to stabilize oil droplets is similar for both pea protein isolates.

Interfacial protein composition may influence droplet interaction with the matrix. The composition of proteins at the droplet interface and the unabsorbed proteins in PPIp and PPId were analysed using SDS-PAGE. Fig. 4B shows the electropherogram of protein composition at the droplet interface and in the aqueous phase of PPIp and PPId under non-reducing conditions. The figure shows that for both PPId and PPIp, the interfacial composition of proteins (PPIp em and PPId em) were similar. In both emulsion, major storage proteins are present at the interface: Legumin at 60, 36 and 20 kDa, and Vicilin at 50, 25 and 16 kDa. Other minor constituents such as convicilin at 70 kDa and enzymes such as lipoxygenase ~90 kDa are also associated with the emulsion droplets (Gatehouse, Croy, Boulter, & Shewry, 1984; O'Kane, Happe, Vereijken, Gruppen, & van Boekel, 2004).

From these results we can conclude that the PPIp and PPId emulsion properties are quite similar, both in term of oil droplet size and protein composition. A similar interfacial composition for both PPIp and PPId emulsions makes it likely that the interactions between proteins in the matrix and interface will be similar in EFGs from both PPIs. The fact that the interfacial composition is similar, implies that differences in interfacial rheology cannot be explained by the composition. This supports our hypothesis that the higher dilatational moduli in PPIp is related to the secondary interaction between protein (aggregates) in the sub-phase and proteins at the interface. Knowing the droplet sizes is also important, as it influences the droplet stiffness and thus the potential of reinforcing the protein network in EFGs. These considerations will be further discussed in the next section.

3.2. Emulsion-filled gels

3.2.1. Small amplitude oscillatory shear (SAOS) rheology

The PPIp and PPId dispersions and protein-enriched emulsions were heated to study their gelling behaviour. Fig. 5 shows the development of G' (elastic modulus) upon heating and cooling as a function of time at pH 7 and pH 5. Upon heating at pH 7 (Fig. 5A) PPIp dispersions and protein-enriched emulsions show a gradual G′ increase, starting around 50 °C. When 95 °C is reached the G′ continues increasing while the temperature remains constant for 10 min. Upon cooling the G′ increases further until 20 °C is reached. The PPIp samples with and without 10 wt % oil, follow similar gelling dynamics at pH 7. At pH 5 (Fig. 5B) the G′ increase of PPIp starts around 80 °C and is more abrupt. Upon cooling the G′ increase is more gradual compared with the increase at pH 7. Another difference between pH 5 and 7, is that at pH 5 the presence of oil causes a reduction of the eventual G′, compared with the PPIp gel without oil. PPId on the other hand, shows an abrupt G′ increase upon heating at pH 7 (Fig. 5A) around a temperature of 60 °C. Then the G′ remains quite constant, until the moment cooling starts. The G′ gradually increases further till a temperature of 20 °C is reached. At pH 5 (Fig. 5B) the G′ increase upon heating is more gradual and more subtle. Also, upon cooling a subtle G' increase is observed. A both pH 7 and 5 oil has little effect on the gelling behaviour of PPId.

The difference between the PPIp and PPId gelling behaviour at pH 7, is that the G′ increase is much more abrupt and pronounced for PPId. The abrupt transition from viscous to gel-like behaviour starts around 60 °C, which is at higher temperature than were the G′ of PPIp starts to increase. This implies that network formation occurs at higher temperatures for PPId than PPIp. The gelation onset temperatures are below their denaturation onset temperature of around 70 °C (Kornet, Shek, et al., 2021, p. 106691), which may be related to the lower heating rate

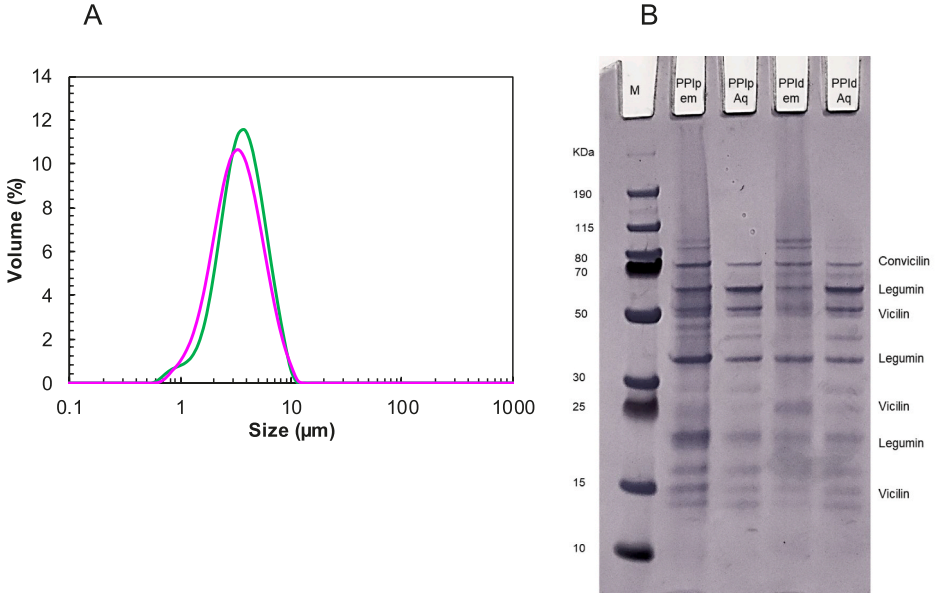

Fig. 4. Representative individual oil droplet size distribution (measured with SDS) of 11.56 wt% oil-in-water emulsion stabilized by 0.02 wt% protein in PPIp (—) and PPId (—) (A); SDS-PAGE of PPIp and PPId stabilized 11.6 wt% oil emulsions at pH 7, with lanes named as follows, M: molecular weight marker, PPIp em.: Interfacial protein profile in PPIp; PPIp Aq.: Aqueous phase protein profile in PPIp; PPId em.: Interfacial protein profile in PPId; PPId Aq.: Aqueous phase protein profile of PPId (B). Identification of the bands is based on earlier research (Gatehouse et al., 1984; O'Kane et al., 2004).

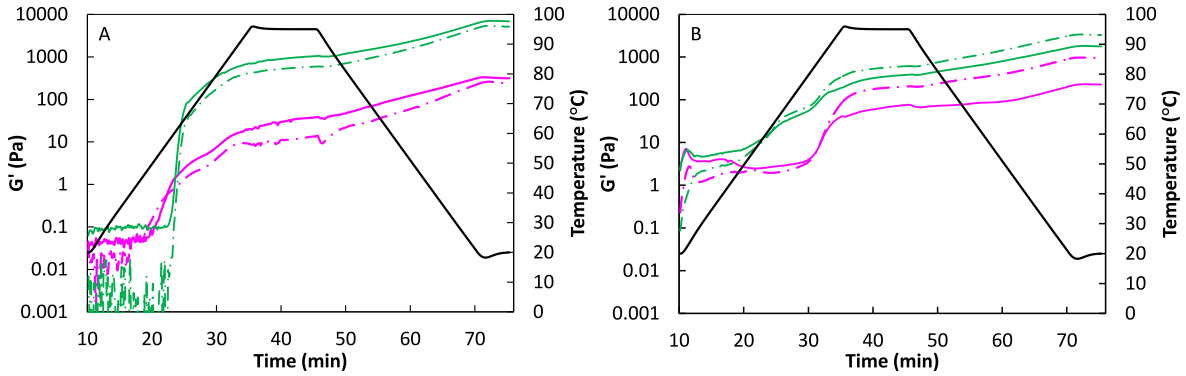

Fig. 5. Temperature sweeps applied on PPIp (—) and PPId (—) dispersions with 15 wt % dry matter (11.3 and 11.7 wt % protein, respectively). The temperature sweeps were also applied on the PPIp and PPId dispersions with 10 wt % oil at pH 7 (A) and pH 5 (B), represented by the dashed lines. All samples were measured in duplicate.

(3 °C/min versus 5 °C/min) and higher protein concentration (15 wt % versus 10 wt % dry matter) in the gelation experiment, compared with the experiment to determine the denaturation temperature (Vermeer & Norde, 2000; Wolz & Kulozik, 2015). The abrupt G′ increase observed for PPId is probably related to the previous observation that it is much less aggregated (i.e., confirmed using DLS) and more soluble (Kornet, Shek, et al., 2021, p. 106691), which may be related to a higher abundance of divalent ions stabilizing the proteins, as well as the milder fractionation process. The high protein solubility allows a more homogeneous distribution of the protein and more freedom to interact with other proteins, as opposed to the more aggregated PPIp. Both PPIp and PPId show a subtle increase in G′ upon cooling, which can be attributed to hydrogen bonding (Sun & Arntfield, 2012). The G′ of PPId after heat-set gelation is around 7 kPa, and is higher than the G' of PPIp, which is around 0.3 kPa. Based on earlier findings (Kornet, Shek, et al., 2021, p. 106691), it is known that the small difference in dispersed protein content (11.7 versus 11.3 wt %) cannot account for this difference in gel firmness. Furthermore, it can be observed from the temperature sweeps that the addition of 10 wt % oil has limited effect on the gelling behaviour of both PPIp and PPId.

At pH 5 (Fig. 5B) PPIp and PPId behave more similar in terms of gelling behaviour. The G′ values before heating are higher compared to those at pH 7, and higher than G", which is indicative of a network already present before heat-set gelation. This network present before heating is probably a result of aggregation, facilitated by a reduced electrostatic repulsion, as the isoelectric point of pea globulins is between pH 4 and 5 (Doan & Ghosh, 2019). In other words, both PPIp and PPId are aggregated before heating and even though aggregation of the pea proteins proceeds further – as demonstrated by the G′ increase upon heating – the effect is more subtle. It is also observed that the final G′ of PPIp becomes slightly higher compared to the final value at pH 7, while the G' of PPId becomes lower than its value at pH 7.

Fig. 6 shows the G′ of the gels as function of the incorporated oil mass fraction at pH 7 (Fig. 6A) and pH 5 (Fig. 6B). At both pH 5 and 7, the G′ does not increase with an increased oil content. This implies that oil does reinforces the gel structures, of neither PPIp nor PPId. At pH 5, there is even an initial decrease until 10 wt % oil, after which G' increases to roughly the same value as compared to the gel without oil. The absence of oil reinforcement either means that oil droplets are less stiff than the matrix, or that the oil droplet interface does not, or weakly, interacts with the gel matrix (Geremias-Andrade et al., 2016; Sala, 2007; Van Vliet, 1988). To estimate the stiffness of the oil droplets Eq. (2) is used with the dilatational elastic modulus (E_d') and the droplet radius (r).

$$G'_{filler} = \frac{2E'_d}{r} \tag{2}$$

Eq. (2) is based on an expression given by van Vliet (1998) with the modification that the surface tension is replaced by the dilatational elastic modulus, after considering the viscoelastic nature of the protein-stabilized interface. Based on the E_d' and r from sections 3.1.1 and 3.1.2, the droplet stiffness was estimated to be around 23 and 15 kPa for PPIp and PPId, respectively. This is higher than the stiffness of the matrix, meaning that in theory these droplets could reinforce the gel structure, if the droplets interact with the matrix and become an integral part of the gel network. Several models have been reported to predict the complex modulus (G*) of soft solids with a continuous matrix and dispersed particles (Manski, Kretzers, Van Brenk, Van der Goot, & Boom, 2007). Two of these models, those of Mooney (1951) and Pal (2002), were tested on their ability to predict the G* of the pea EFGs (Mooney, 1951; Pal, 2002). It turned out that the models were not suitable to

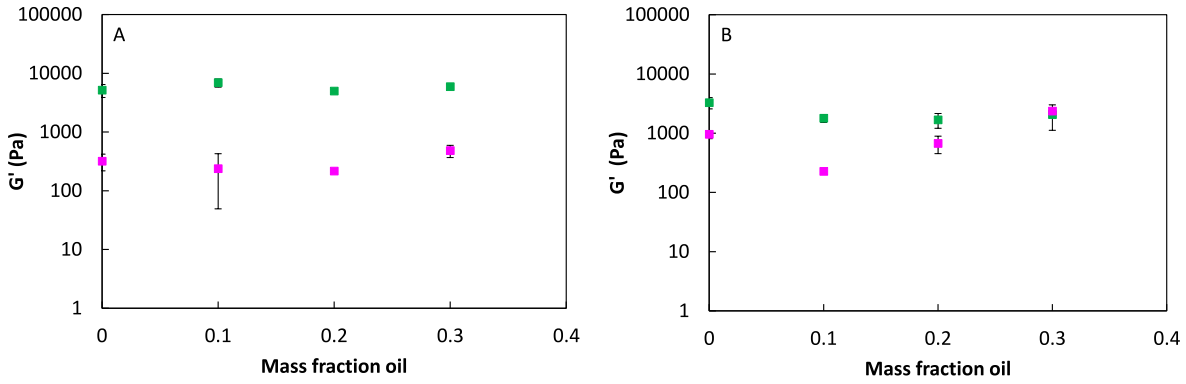

Fig. 6. Gel firmness (G′) as function of mass fraction oil of PPIp (■) and PPId (■) at pH 7 (A) and pH 5 (B). All samples were measured in duplicate and standard deviations are shown.

predict the complex moduli of the samples in this study, partially because the overall G' differences at different oil contents were small. This suggests that oil does not reinforce the pea protein gels, probably due to weak interactions between droplet interface and matrix. It can be hypothesized that the proteins at the interface orient themselves in such a way that most hydrophobic patches are in the oil phase, making them unavailable for hydrophobic interactions with neighbouring proteins at the interface or bulk upon heat-induced gelation.

It is noted that the lack of oil reinforcement is also specific to the sample conditions tested. This is nicely illustrated by the study of Silva et al. (2019), who observed that at different conditions (i.e., 4 wt % protein, pH 5.8) oil could be used to increase the stiffness of emulsions upon heating (Silva et al., 2019). This implies that in pea protein emulsions, oil may in fact be able to increase the stiffness, even though it cannot reinforce pea protein emulsion-filled gels.

3.2.2. *Medium and large amplitude oscillatory shear rheology*

The heat-set gels and emulsion-filled gels were further characterized by medium and large amplitude oscillatory shear (MAOS & LAOS) rheology. From the sinusoidal waveform data at each strain amplitude the energy dissipation ratio was calculated. The energy dissipation ratio is the dissipated energy within one cycle divided by the dissipation of an ideally plastic material. This ratio reflects the dissipated energy at a certain deformation – with a purely elastic response when $\Phi = 0$ and a perfectly plastic response when $\Phi = 1$ (Ptaszek, 2014) – and hence provides a compact overview of its breakdown behaviour.

Fig. 7 shows the energy dissipation ratios (EDR) of PPIp and PPId without oil and with 10 wt % oil, as a function of strain amplitude Fig. 7A shows an increase of the EDR at around 10% strain for PPIp gels without oil. When oil was present the EDR already increased at lower strain. After reaching 10% strain, the viscous dissipation of the PPIp gel with 10 wt % oil increased much faster with increasing strain. This implies that the addition of oil made the PPIp gels at pH 7 more brittle. The lack of oil reinforcement could be due to weak oil droplet – protein matrix interactions, which also aligns with the interfacial rheology, where in-plane protein interactions were found to be weak. This weak interaction would disrupt the bulk protein-protein interactions and cause break down at lower strain, reflected in an increased brittleness.

The difference at pH 5 (Fig. 7B) between PPIp gels with and without oil was much smaller, as the EDRs showed a similar trend. Also, viscous dissipation became significant at much larger strain, compared with the PPIp gels at pH 7. This means that at pH 5 the PPIp gels were more ductile, compared with the PPIp gels at pH 7. The PPId gels at pH 7 showed a significant EDR increase at around 30% strain (Fig. 7A). This was also the case for the PPId gel with 10 wt % oil, which implies that oil had little effect on the response to large deformation of PPId gels at pH 7. The same is true at pH 5 (Fig. 7B), where little difference was observed between the PPId gels with and without oil. Compared with pH 7, the EDR at pH 5 started to increase at lower strain but evolved more gradually. PPIp gels showed an earlier increase in dissipation ratio than PPId, at pH 7. This indicates that PPIp (emulsion-filled) gels were more brittle, probably because of the weakly-connected network of pre-formed protein aggregates. Also, a major difference was seen between the PPIp gel and the emulsion-filled gel (10 wt % oil), as the latter showed significantly more viscous dissipation at a lower strain. This indicates that oil weakens the PPIp gel structure at pH 7, which may be related to oil occupying the interstitial space between protein aggregates and consequently a decreased interaction between these aggregates. Another difference between PPIp and PPId is that the breakdown behaviour is more gradual for PPIp and more abrupt for PPId. The more gradual breakdown of PPIp is probably related to a more heterogeneous network, leading to a spectrum of interactions, that are broken at different extents of deformation. This heterogeneity was already observed for heat-set gels at pH 7 in a previous study (Kornet, Shek, et al., 2021, p. 106691) and will further be discussed in section 3.2.3 for the EFGs. At pH 5 (Fig. 7B) the breakdown behaviour of PPId became more gradual and more comparable with PPIp. This can be explained by the fact that close to the isoelectric point of pea protein, PPId now also forms leads to a heterogeneous gel network just like PPIp.

A more detailed overview of the gel responses to large deformation is given in Fig. 8, where Lissajous plots at three strain amplitudes within the MAOS (medium amplitude oscillatory shear) regime are shown. The top panel of this figure shows the elastic Lissajous plots of stress versus strain for PPIp (left) and PPId (right) gel matrix and emulsion-filled gels with 10 wt % oil at pH 7 (black) and pH 5 (green).

The left panel shows a clear difference between PPIp at pH 7 and pH 5. Already at 50% strain the gels at pH 7 display a somewhat rhomboidal shape, indicating a predominantly viscous response, whereas at pH 5 they show a more elastic strain stiffening response (indicated by the increased slope of the stress at higher strain). This strain stiffening persists in the MAOS regime until 100% strain deformation. In line with Fig. 7, it shows that PPIp has higher stretchability at pH 5, compared with pH 7, and here we also see a strain stiffening response at medium amplitude. A similar observation is seen in the viscous Lissajous plots (bottom row for PPIp), where the Lissajous plots representing the gels at pH 5, remain wider over the MAOS strain amplitude range.

In the right panels of Fig. 8 the elastic and viscous Lissajous plots for PPId gels and emulsion-filled gels (10 wt % oil) are shown. It can be observed that the non-linear response in the MAOS regime is much more similar at pH 5 and 7, compared with PPIp gels. Even though the gel stiffness of PPId gels decreased at pH 5, the nonlinear response remained quite similar. At 100% strain the Lissajous plots representing the gels at pH 5 become wider, indicating a more viscous response. This is consistent with Fig. 7, where the energy dissipation ratio increased at a somewhat lower strain. At a strain of 50% the gels at pH 5 and 7 still behaved nearly identical with a strain stiffening response, indicated by the increase in stress near the maximum strain. Also, the response in the viscous Lissajous plots was similar between pH 5 and 7, with a transition to a rhomboidal shape at 50% strain amplitude and a narrower more sigmoidal-shaped curve at 100% strain amplitude. The overall narrowing indicates a transition towards a more viscous response, and the sigmoidal shape seen at larger strain is indicative of strain-thinning

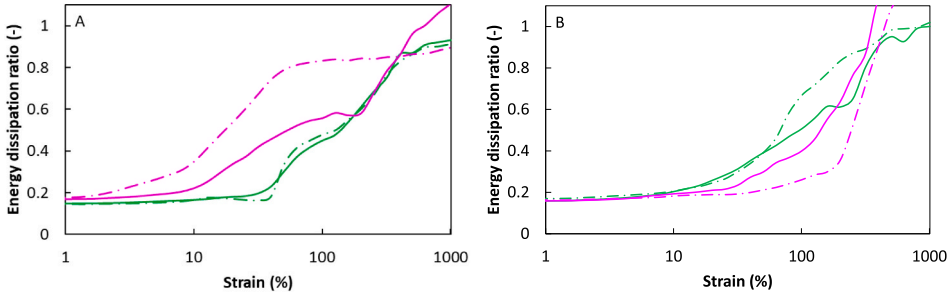

Fig. 7. Average energy dissipation ratios of PPIp (—) and PPId (—) gels without oil (15 wt % PPI) and PPIp and PPId gels with oil (15 wt % PPI, 10 wt % oil), represented by the dashed lines. The samples were measured at pH 7 (A) and pH 5 (B).

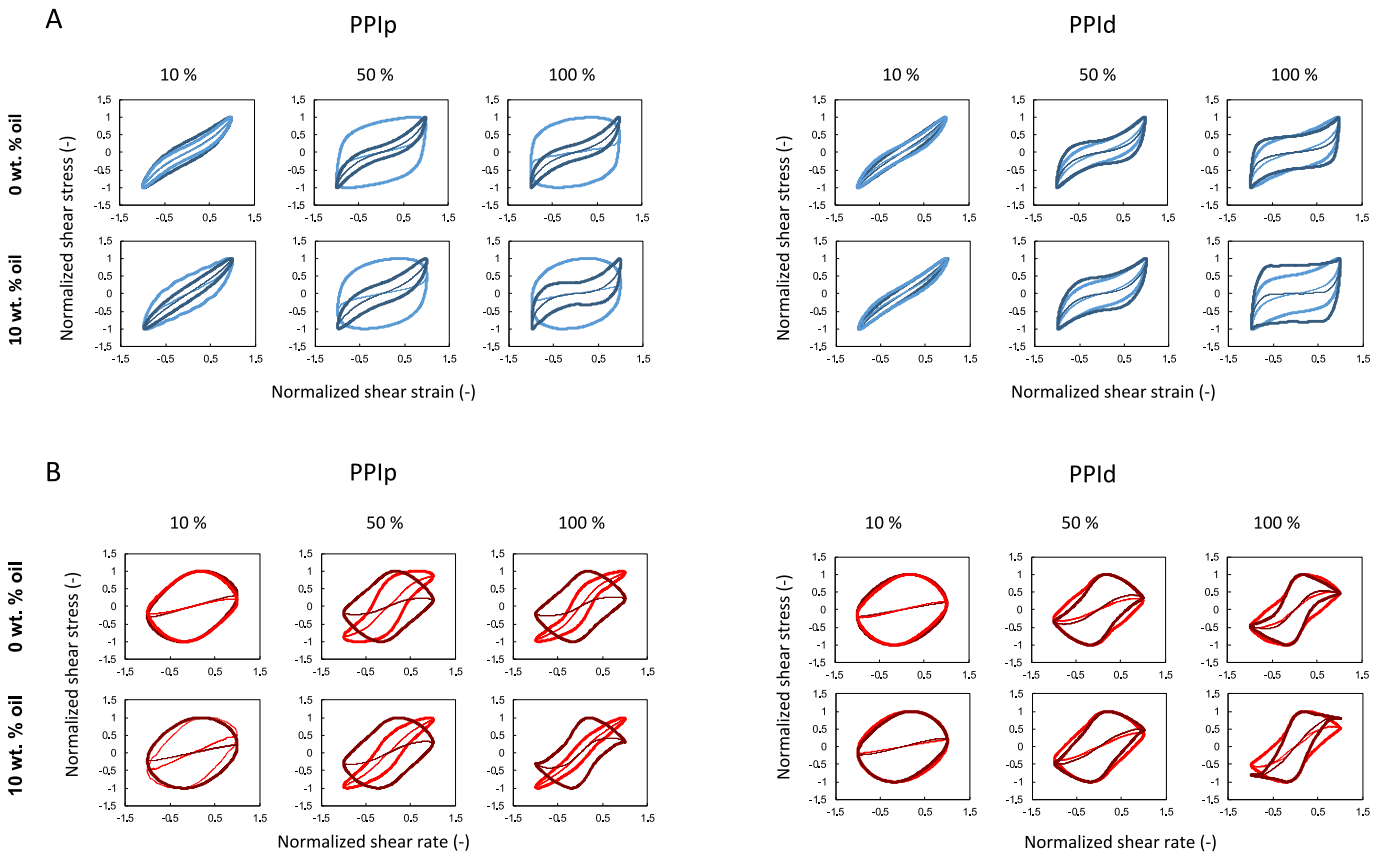

Fig. 8. Elastic Lissajous plots of stress versus strain for PPIp and PPId gels without oil (15 wt % PPI) and with oil (15 wt % PPI, 10 wt % oil) at pH 5 (—) and 7 (—) and B. viscous Lissajous plots of stress versus strain rate at pH 5 (—) and 7 (—). The response at 10, 50 and 100% strain deformation are shown. The strain, stress and strain rate axis values are normalized (min-max normalization).

behaviour. A similar transition from predominantly elastic to a viscous behaviour was seen for gels from high concentrations of debranched starch (Precha-Atsawanan, Uttapap, & Sagis, 2018).

In conclusion, it appeared that PPId gels are more ductile and less influenced by pH, in their response to large deformation compared with PPIp gels. Gels and emulsion-filled gels from PPIp showed higher deformability at pH 5 compared with pH 7. These results again show that plant protein isolates from the same protein source can display different functional behaviour, depending on the method of fractionation.

3.2.3. *Microstructure of emulsion-filled gels*

Microscopic analysis of the gels can provide further visual information on the microstructure to support and explain rheological behaviour. Therefore, multi photon microscopy was employed to visualize the microstructure of gels and the EFGs. Fig. 9 shows confocal images of PPIp and PPId matrices and EFG with 10 wt% oil after heating at both pH 7 and pH 5. The figure also shows 3D construct of the matrix of all four samples. The green fluorescence represents proteins, and the red fluorescence represents oil droplets.

The images of PPIp at pH 7 (1st row) show a patchy distribution of protein aggregates (green). The 3D image of the matrix also indicates that the protein network is highly heterogeneous and constituted of protein aggregates with a wide range of sizes. In PPId at pH 7 (2nd row), the protein network is more homogenous on a microscale and is void of large protein aggregates. The 3D image of the matrix also indicates that PPId forms a more cohesive homogeneous network, in stark contrast to PPIp at pH 7. This is also reflected in the rheology of the matrix, which shows that PPId (G': ~5000 Pa) forms a firmer gel compared to PPIp (G': ~500 Pa). The addition of oil droplets in both PPIp and PPId matrix (EFGs) does not change the microstructure compared to the matrix. The oil droplets also do not seem to be incorporated within the protein network, as the protein concentration at the oil droplet interface does not appear higher than in the matrix. The microstructural analysis in combination with the negligible effect on G′ upon addition of oil (Fig. 5) indicates that the oil droplets, simply act as inert fillers. The image of the PPIp matrix at pH 5 (3rd row) indicates that the protein network is still constituted of a heterogeneous protein network. This microstructure is more evident in the 3D image of the matrix. The microstructure protein aggregates seem smaller and more homogeneous than at pH 7. This is also related to the higher G′ values of PPIp at pH 5, compared with PPIp at pH 7. Moreover, the gel at pH 5 remains predominantly elastic for much larger strains (~100%) compared to pH 7 (~10%). On the other hand, in PPId at pH 5 (4th row), the microstructure was much different from PPId at pH 7. The PPId matrix formed a more aggregated protein network as opposed to a homogenous, cohesive network, which may explain the lower G′ values at pH 5. The EFG images of PPIp at pH 5 indicate that the oil droplets were distributed evenly throughout the protein network. This means that the oil droplets evenly occupied the interstitial space between the protein network on microscale, which could be related to the slight 'G' increase at higher oil concentrations seen for PPIp EFGs at pH 5 (Fig. 6). In PPId at pH 5, the addition of oil (EFGs), did not contribute to an increase in EFG firmness. The oil droplets do not seem to be incorporated into the protein network, so they could also be considered inert fillers.

Overall, pea protein EFGs show different microstructural and rheological characteristics. At pH 7, PPId clearly formed more ductile and cohesive protein gels and EFGs compared with PPIp. In both cases, the incorporation of oil droplets (EFGs), did not reinforce the protein matrix. At pH 5, both PPIp and PPId formed gels and EFGs with similar

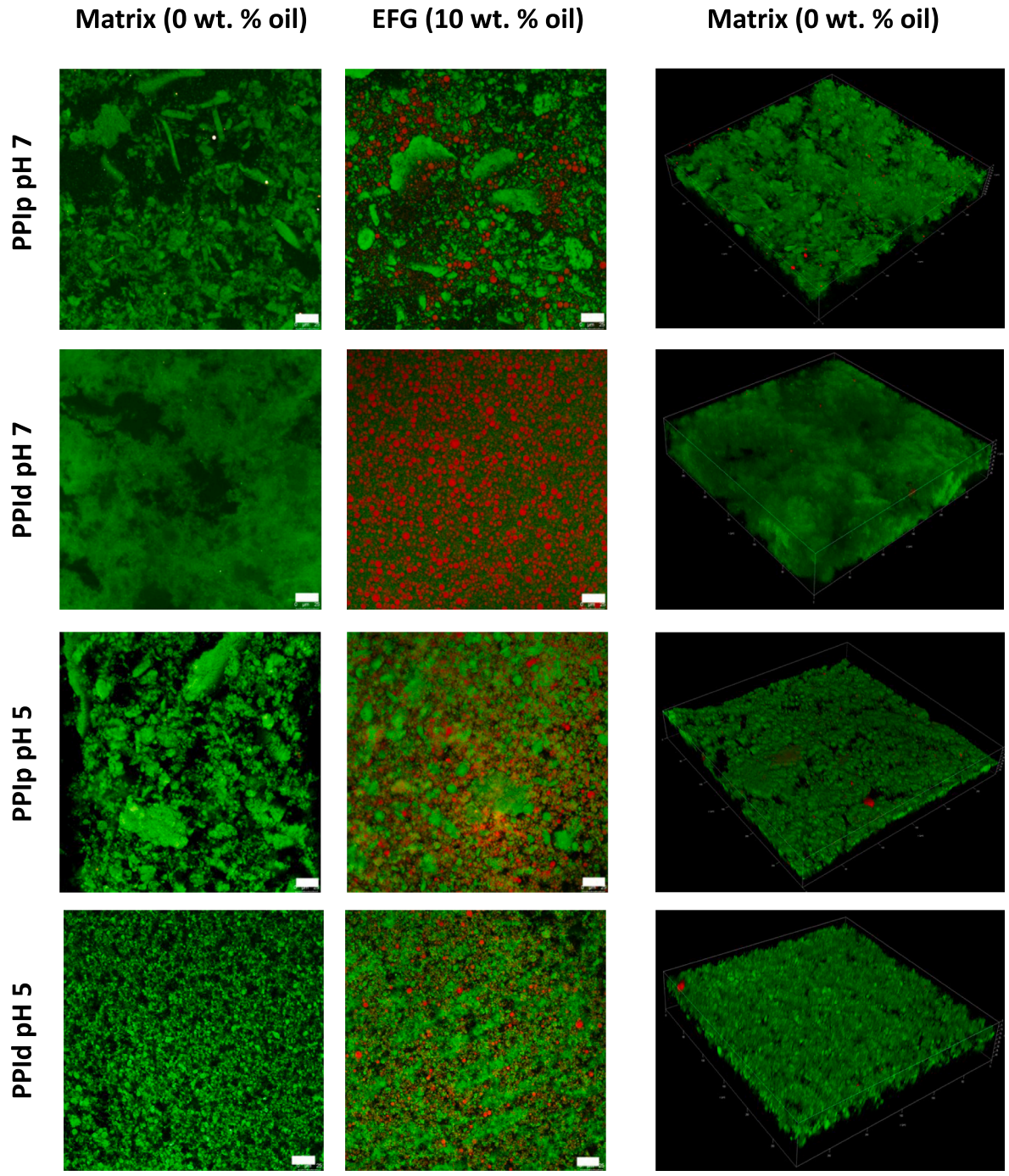

Fig. 9. Multi photon microscope images of PPIp (precipitated) and PPId (diafiltrated) gels without oil (15 wt % PPI) and gels with oil (15 wt % PPI, 10 wt % oil) at pH 7 and pH 5 with Nile Red for the oil (red) and Fast Green for proteins (green). (For interpretation of the references to colour in this figure legend, the reader is referred to the Web version of this article.)

firmness. So, for PPIp, the gels became firmer at pH 5 compared with pH 7 and for PPId, the gels became slightly weaker at pH 5 compared with pH 7. The difference in microstructure and rheological behaviour between the two PPIs stems from the different fractionation routes used to obtain them. PPIp is fractionated using isoelectric precipitation, which caused some proteins to undergo irreversible aggregation. At pH 7, these process-induced aggregates further grow upon heating to form patchy, weaker PPIp EFGs. In PPId, the proteins are not subjected to aggregation during fractionation, leading to more soluble proteins. The more soluble proteins in PPId form a cohesive network upon heating. Such a cohesive network leads to a more homogeneous distribution of oil droplets and to the formation of firmer gels and EFGs.

4. Conclusion

In this study, we compared two pea protein isolates that were obtained using different fractionation routes: one fractionated by isoelectric precipitation (PPIp) and the other by diafiltration (PPId). Despite of having a different gelling behaviour, it appeared that both pea protein isolates behaved rather similar in terms of emulsifying and interfacial properties. When the emulsions were used to form emulsion-filled gels (EFGs), differences in gelling behaviour were seen, which could be

largely attributed to the different fractionation routes. Although both pea protein isolates could form emulsion-filled gels at pH 5 and 7, it appeared that diafiltrated pea protein isolate formed firmer gels and emulsion-filled gels than isoelectric precipitated pea protein isolate. Lowering the pH to 5 however, was beneficial for PPIp in terms of emulsion-filled gel firmness, whereas this was not the case for PPId. Moreover, oil did not play an active role in terms of gel reinforcement for any of the EFGs. This indicates a weak protein-protein interaction between the oil droplets and the pea protein matrix, as we also observed weak in-plane interactions at the interface.

The observation that pea protein isolates can form emulsion-filled gels could be relevant for food applications, such as plant-based cheeses and meat analogues. Our observations also reiterate the importance of processing routes when using plant proteins for such applications. For instance, from our observations, it was found that PPId form firmer gels at pH 7, also in the presence of oil droplets (EFGs), compared to PPIp. However, if the application desires to produce EFGs at pH 5, PPIp or PPId form almost equally firm gels, especially in the presence of oil droplets. Therefore, we show that the fractionation process plays a significant role in the properties of pea protein stabilized emulsion-filled gels, and that such effect is also pH dependent. The insights from this study may contribute to the design of pea protein fractionation routes that are tailored to the food product conditions and the type of gel envisioned.

Author statement

Remco Kornet: Conceptualization, Methodology, Investigation, Validation, Visualization, Writing – Original Draft. **Simha Sridharan:** Conceptualization, Methodology, Investigation, Validation, Visualization, Writing – Original Draft. **Paul Venema:** Supervision, Writing – Review & Editing. **Leonard Sagis**: Writing – Review & Editing. **Constantinos V. Nikiforidis:** Supervision, Writing – Review & Editing. **Atze Jan van der Goot:** Writing – Review & Editing. **Marcel Meinders:** Supervision, Writing – Review & Editing. **Erik van der Linden:** Writing – Review & Editing, Funding Acquisition.

Declaration of competing interest

The authors have declared that no competing interests exist.

Acknowledgements

The authors want to thank Helene Mocking-Bode and Irene van den Hoek for their contribution in obtaining the pea protein fractions. This research project is organised by and executed under the auspices of TiFN, a public - private partnership on precompetitive research in food and nutrition. The authors have declared that no competing interests exist in the writing of this publication. Funding for this research was obtained from Unilever Research and Development Wageningen., Nutricia Research B·V., Bel S.A., Pepsico Inc., and the Top sector Agri & Food.

References

Adenekan, M. K., Fadimu, G. J., Odunmbaku, L. A., & Oke, E. K. (2018). Effect of isolation techniques on the characteristics of pigeon pea (Cajanus cajan) protein isolates. *Food Sciences and Nutrition, 6*(1), 146–152.

Alonso-Miravalles, L., Jeske, S., Bez, J., Detzel, A., Busch, M., Krueger, M., et al. (2019). Membrane filtration and isoelectric precipitation technological approaches for the preparation of novel, functional and sustainable protein isolate from lentils. *European Food Research and Technology, 245*(9), 1855–1869.

Beverung, C., Radke, C. J., & Blanch, H. W. (1999). Protein adsorption at the oil/water interface: Characterization of adsorption kinetics by dynamic interfacial tension measurements. *Biophysical Chemistry, 81*(1), 59–80.

Boukid, F., Rosell, C. M., & Castellari, M. (2021). Pea protein ingredients: A mainstream ingredient to (re) formulate innovative foods and beverages. *Trends in Food Science & Technology, 110*, 729–742.

Burger, T. G., & Zhang, Y. (2019). Recent progress in the utilization of pea protein as an emulsifier for food applications. *Trends in Food Science & Technology, 86*, 25–33.

Doan, C. D., & Ghosh, S. (2019). Formation and stability of pea proteins nanoparticles using ethanol-induced desolvation. *Nanomaterials, 9*(7), 949.

Ewoldt, R. H., Winter, P., Maxey, J., & McKinley, G. H. (2010). Large amplitude oscillatory shear of pseudoplastic and elastoviscoplastic materials. *Rheologica Acta, 49*(2), 191–212.

Farjami, T., & Madadlou, A. (2019). An overview on preparation of emulsion-filled gels and emulsion particulate gels. *Trends in Food Science & Technology, 86*, 85–94.

Fuhrmeister, H., & Meuser, F. (2003). Impact of processing on functional properties of protein products from wrinkled peas. *Journal of Food Engineering, 56*(2–3), 119–129.

Gatehouse, J. A., Croy, R. R., Boulter, D., & Shewry, P. R. (1984). The synthesis and structure of pea storage proteins. *Critical Reviews in Plant Sciences, 1*(4), 287–314.

Geremias-Andrade, I. M., Souki, N. P., Moraes, I. C., & Pinho, S. C. (2016). Rheology of emulsion-filled gels applied to the development of food materials. *Gels, 2*(3), 22.

Hinderink, E. B., Münch, K., Sagis, L., Schroën, K., & Berton-Carabin, C. C. (2019). Synergistic stabilisation of emulsions by blends of dairy and soluble pea proteins: Contribution of the interfacial composition. *Food Hydrocolloids, 97*, Article 105206.

Jose, J., Pouvreau, L., & Martin, A. H. (2016). Mixing whey and soy proteins: Consequences for the gel mechanical response and water holding. *Food Hydrocolloids, 60*, 216–224.

Jung, S., Lamsal, B., Stepien, V., Johnson, L., & Murphy, P. (2006). Functionality of soy protein produced by enzyme-assisted extraction. *Journal of the American Oil Chemists' Society, 83*(1), 71–78.

Karaca, A. C., Low, N., & Nickerson, M. (2011). Emulsifying properties of chickpea, faba bean, lentil and pea proteins produced by isoelectric precipitation and salt extraction. *Food Research International, 44*(9), 2742–2750.

Kim, K., Renkema, J., & Van Vliet, T. (2001). Rheological properties of soybean protein isolate gels containing emulsion droplets. *Food Hydrocolloids, 15*(3), 295–302.

Kiosseoglou, A., Doxastakis, G., Alevisopoulos, S., & Kasapis, S. (1999). Physical characterization of thermally induced networks of lupin protein isolates prepared by isoelectric precipitation and dialysis. *International Journal of Food Science and Technology, 34*(3), 253–263.

Kornet, R., Shek, C., Venema, P., Goot, A. J.v. d., Meinders, M., & Linden, E.v. d. (2021). Substitution of whey protein by pea protein is facilitated by specific fractionation routes. *Food Hydrocolloids*, Article 106691.

Kornet, R., Veenemans, J., Venema, P., Goot, A. J.v. d., Meinders, M., Sagis, L., et al. (2021). Less is more: Limited fractionation yields stronger gels for pea proteins. *Food Hydrocolloids, 112*, Article 106285.

Kornet, R., Venema, P., Nijsse, J., Linden, E.v. d., Goot, A. J.v. d., & Meinders, M. (2020). Yellow pea aqueous fractionation increases the specific volume fraction and viscosity of its dispersions. *Food Hydrocolloids, 99*, Article 105332.

Kornet, R., Penris, S., Venema, P., van der Goot, A. J., Meinders, M. B. J., & van der Linden, E. (2021). How pea fractions with different protein composition and purity can substitute WPI in heat-set gels. *Food Hydrocolloids, 120*, 106891.

Larson, A. M. (2011). Multiphoton microscopy. *Nature Photonics, 5*(1), 1-1.

Makri, E., Papalamprou, E., & Doxastakis, G. (2005). Study of functional properties of seed storage proteins from indigenous European legume crops (lupin, pea, broad bean) in admixture with polysaccharides. *Food Hydrocolloids, 19*(3), 583–594.

Manski, J., Kretzers, I., Van Brenk, S., Van der Goot, A., & Boom, R. (2007). Influence of dispersed particles on small and large deformation properties of concentrated caseinate composites. *Food Hydrocolloids, 21*(1), 73–84.

McCann, T. H., Guyon, L., Fischer, P., & Day, L. (2018). Rheological properties and microstructure of soy-whey protein. *Food Hydrocolloids, 82*, 434–441.

Mooney, M. (1951). The viscosity of a concentrated suspension of spherical particles. *Journal of Colloid Science, 6*(2), 162–170.

Ntone, E., van Wesel, T., Sagis, L. M. C., Meinders, M., Bitter, J. H., & Nikiforidis, C. V. (2020). Adsorption of rapeseed proteins at oil/water interfaces. Janus-like napins dominate the interface. *Journal of Colloid and Interface Science, 583*, 459–469.

O'Kane, F. E., Happe, R. P., Vereijken, J. M., Gruppen, H., & van Boekel, M. A. (2004). Characterization of pea vicilin. 1. Denoting convicilin as the α-subunit of the Pisum vicilin family. *Journal of Agricultural and Food Chemistry, 52*(10), 3141–3148.

Pal, R. (2002). Complex shear modulus of concentrated suspensions of solid spherical particles. *Journal of Colloid and Interface Science, 245*(1), 171–177.

Panyam, D., & Kilara, A. (1996). Enhancing the functionality of food proteins by enzymatic modification. *Trends in Food Science & Technology, 7*(4), 120–125.

Papalamprou, E., Doxastakis, G., Biliaderis, C., & Kiosseoglou, V. (2009). Influence of preparation methods on physicochemical and gelation properties of chickpea protein isolates. *Food Hydrocolloids, 23*(2), 337–343.

Pelgrom, P. J. M., Vissers, A. M., Boom, R. M., & Schutyser, M. A. I. (2013). Dry fractionation for production of functional pea protein concentrates. *Food Research International, 53*(1), 232–239.

Peng, Y., Kersten, N., Kyriakopoulou, K., & van der Goot, A. J. (2020). Functional properties of mildly fractionated soy protein as influenced by the processing pH. *Journal of Food Engineering, 275*, Article 109875.

Precha-Atsawanan, S., Uttapap, D., & Sagis, L. M. (2018). Linear and nonlinear rheological behavior of native and debranched waxy rice starch gels. *Food Hydrocolloids, 85*, 1–9.

Ptaszek, P. (2014). Large amplitudes oscillatory shear (Laos) behavior of egg white foams with apple pectins and xanthan gum. *Food Research International, 62*, 299–307.

Sagis, L. M., & Scholten, E. (2014). Complex interfaces in food: Structure and mechanical properties. *Trends in Food Science & Technology, 37*(1), 59–71.

Sala, G. (2007). *Food gels filled with emulsion droplets: Linking large deformation properties to sensory perception*.

Sala, G., Van Aken, G. A., Stuart, M. A. C., & Van De Velde, F. (2007). Effect of droplet–matrix interactions on large deformation properties of emulsion-filled gels. *Journal of Texture Studies, 38*(4), 511–535.

Schmitt, C., Silva, J. V., Amagliani, L., Chassenieux, C., & Nicolai, T. (2019). Heat-induced and acid-induced gelation of dairy/plant protein dispersions and emulsions. *Current Opinion in Food Science, 27*, 43–48.

Shand, P. J., Ya, H., Pietrasik, Z., & Wanasundara, P. K. J. P. D. (2007). Physicochemical and textural properties of heat-induced pea protein isolate gels. *Food Chemistry, 102*(4), 1119–1130.

Sikorski, Z. E. (2001). Functional properties of proteins in food systems. *Chemical and Functional Properties of Food Proteins*, 113–135.

Silva, J. V., Jacquette, B., Amagliani, L., Schmitt, C., Nicolai, T., & Chassenieux, C. (2019). Heat-induced gelation of micellar casein/plant protein oil-in-water emulsions. *Colloids and Surfaces A: Physicochemical and Engineering Aspects, 569*, 85–92.

Sridharan, S., Meinders, M. B., Bitter, J. H., & Nikiforidis, C. V. (2020). Pea flour as stabilizer of oil-in-water emulsions: Protein purification unnecessary. *Food Hydrocolloids, 101*, Article 105533.

Stone, A. K., Karalash, A., Tyler, R. T., Warkentin, T. D., & Nickerson, M. T. (2015). Functional attributes of pea protein isolates prepared using different extraction methods and cultivars. *Food Research International, 76*, 31–38.

Sun, X. D., & Arntfield, S. D. (2011). Gelation properties of salt-extracted pea protein isolate induced by heat treatment: Effect of heating and cooling rate. *Food Chemistry, 124*(3), 1011–1016.

Sun, X. D., & Arntfield, S. D. (2012). Molecular forces involved in heat-induced pea protein gelation: Effects of various reagents on the rheological properties of salt-extracted pea protein gels. *Food Hydrocolloids, 28*(2), 325–332.

Tang, C.-H., Chen, L., & Foegeding, E. A. (2011). Mechanical and water-holding properties and microstructures of soy protein isolate emulsion gels induced by CaCl2, glucono-δ-lactone (GDL), and transglutaminase: Influence of thermal treatments before and/or after emulsification. *Journal of Agricultural and Food Chemistry, 59*(8), 4071–4077.

Tangsuphoom, N., & Coupland, J. N. (2008). Effect of surface-active stabilizers on the microstructure and stability of coconut milk emulsions. *Food Hydrocolloids, 22*(7), 1233–1242.

Van Vliet, T. (1988). Rheological properties of filled gels. Influence of filler matrix interaction. *Colloid & Polymer Science, 266*(6), 518–524.

Vermeer, A. W., & Norde, W. (2000). The thermal stability of immunoglobulin: Unfolding and aggregation of a multi-domain protein. *Biophysical Journal, 78*(1), 394–404.

Vestergaard, M., Chan, S. H. J., & Jensen, P. R. (2016). Can microbes compete with cows for sustainable protein production-A feasibility study on high quality protein. *Scientific Reports, 6*(1), 1–8.

Wolz, M., & Kulozik, U. (2015). Thermal denaturation kinetics of whey proteins at high protein concentrations. *International Dairy Journal, 49*, 95–101.

Yang, M., Liu, F., & Tang, C.-H. (2013). Properties and microstructure of transglutaminase-set soy protein-stabilized emulsion gels. *Food Research International, 52*(1), 409–418.

Zeeb, B., McClements, D. J., & Weiss, J. (2017). Enzyme-based strategies for structuring foods for improved functionality. *Annual Review of Food Science and Technology, 8*, 21–34.